Conf-9010243--7

CONF-9010243--7

DE91 006360

Analysis of a Drum Chopper for Use on a New Small Angle Diffractometer at IPNS*

R. K. Crawford, J. E. Epperson, P. Thiyagarajan, and J. M. Carpenter

Argonne National Laboratory, Argonne, IL 60439.

To be Presented at

The International Collaboration on Advanced Neutron Sources, ICANS-XI Meeting

Tsukuba, Japan

October 22-26, 1990

*Work supported by U.S. Department of Energy, BES, contract No. W-31-109-ENG-38

Analysis of a Drum Chopper for Use on a New Small Angle Diffractometer at IPNS*

R. K. Crawford, J. E. Epperson, P. Thiyagarajan, and J. M. Carpenter
Argonne National Laboratory, Argonne, IL 60439.

ABSTRACT

Light-weight drum choppers rotating at 15 Hz have been in use on the IPNS powder diffractometers for several years, where they serve to eliminate the delayed-neutron background from much of the spectral region of interest. Monte Carlo simulations indicate that a similar chopper operated at 15 Hz should do an excellent job of delayed-neutron removal in the new small-angle diffractometer being designed at IPNS. The simulations also show that when the same chopper is operated at 7.5 Hz it performs quite successfully as a frame-elimination chopper, effectively eliminating neutrons from alternate pulses and allowing extension of the useful wavelength range of the instrument to ~28 Å. Thus the incorporation of such a chopper should add considerably to the range and flexibility of the new instrument.

I. INTRODUCTION

A major goal in the design of a new small-angle diffractometer at IPNS is the achievement of a much lower Q_{min} than is currently available on the IPNS small-angle diffractometer SAD (current Q_{min} for SAD is ~0.005 $Å^{-1}$). Since

$$Q = (4\pi \sin\theta)/\lambda , \qquad (1)$$

reaching smaller values of Q means measuring either to smaller values of the scattering angle $\phi=2\theta$ or to larger values of the wavelength λ, or both. Practical considerations require that the total source-detector distance be at least ~9 m, so that wavelengths beyond ~14 Å are overtaken by neutrons from the next frame of the 30 Hz source. Thus access to wavelengths longer than 14 Å on the new instrument will require the use of some means of either a) eliminating all wavelengths shorter than 14 Å or b) eliminating alternate source pulses. This paper addresses the feasibility of the latter approach.

*Work supported by U.S. Department of Energy, BES, contract No. W-31-109-ENG-38.

A significant problem at pulsed spallation neutron sources using fissionable material in their targets is the "delayed" neutrons which are emitted from short-lived excited states of the target nuclei.[1,2] Because the lifetimes of these excited states range up to tens of seconds, these delayed neutrons leave the target at times which are uncorrelated with the prompt pulses, and so cannot be energy-analyzed by the usual time-of-flight (TOF) methods. Instead they contribute to the sample-dependent background in the neutron scattering instruments. Broad-bandpass neutron choppers have been used to reduce the delayed-neutron background on the IPNS powder diffractometers SEPD and GPPD for the past two years.[3] They have been very successful in reducing this background in the long-wavelength regions of the TOF spectrum, where the scattering signal is usually the weakest and hence background is most troublesome. A similar chopper should likewise be effective in reducing the delayed-neutron background in small-angle diffractometers at pulsed neutron sources.

A simulation program has been written to assess the use of a chopper similar to those used for delayed-neutron removal at SEPD and GPPD to eliminate alternate source pulses, and to study the quality of the small-angle scattering data which results under these conditions. This simulation allows the treatment of delayed neutrons, so the ability of such a chopper to reduce the delayed-neutron background can also be assessed. The simulation program and the results obtained are discussed below. A semi-quantitative comparison between this use of a frame-elimination chopper to access larger values of λ to reach small Q and the alternative of using tighter collimation to allow measurements to smaller values of ϕ to reach the same small Q is also included so that the relative data rates available under the two different approaches might be estimated.

Although the simulation results reported here are specific to the geometries of the IPNS small-angle diffractometers and to the 30 Hz IPNS source repetition rate, the resulting conclusions should be qualitatively applicable to any other pulsed-source small-angle diffractometer where the source pulsing frequency is higher than optimum. Calculations of this type could be readily adapted to other instrument geometries and source frequencies if quantitative information is desired in those cases.

II. THE SIMULATION

The program FECHOPS is a Monte Carlo simulation of a small-angle scattering instrument which was designed to provide a detailed understanding of the effects which would occur if a drum chopper, similar to those used for delayed neutron removal on the powder diffractometers SEPD and GPPD at IPNS, were used to remove the delayed neutrons or to "eliminate" alternate prompt pulses to permit the utilization of long-wavelength neutrons. FECHOPS was modeled after the earlier program DNCHOP[4] which was developed to analyze the use of delayed-neutron choppers on SEPD and GPPD. The geometry for this simulation is shown in Fig. 1, and Appendix 1 develops the equations governing such a drum chopper.

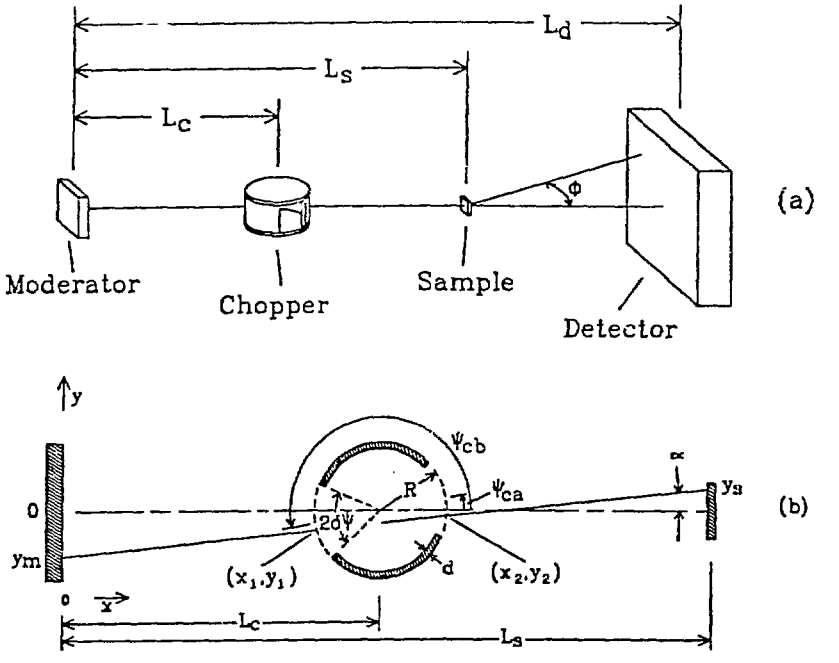

Figure 1. a) Schematic layout of moderator, chopper, sample, and detector used for this simulation. b) Details of chopper geometry.

Neutron Trajectories

The simulation considered neutrons arriving at the detector over two "frames" of the 30 Hz source, or 66667 μs, with the frame-1 prompt pulse occurring at the beginning of this period. FECHOPS generated a set of neutron trajectories from moderator to detector. Each trajectory was analyzed according to whether it was intercepted and/or absorbed by the chopper and according to whether it represented a neutron which would be detected by a real detector. It was also analyzed according to whether it originated from the prompt pulse of frame-1, the prompt pulse of frame-2, or as a delayed neutron. (Delayed neutrons were assumed to be uniformly distributed in time, and to have the same energy spectrum as the prompt neutrons.) Each trajectory was along a line in the x,y plane from a random point on the moderator through a random point on the sample (see Fig. 1), so that the full ranges of relevant angles and positions at the chopper were sampled. For most of the simulations the chopper was operated to pass a broad band of the neutrons originating in the frame-1 prompt pulse, while eliminating most neutrons originating in the frame-2 prompt pulse which occurred 33333 μs after the frame-1 pulse. Figure 2 shows a distance *vs* time diagram for the chopper and pulsed source operating under these conditions. Figure 3 shows the operation of the chopper at twice this frequency in a purely delayed-neutron-removal mode where it is set to pass a broad band of wavelengths from each prompt pulse of the source. Both drawings also show sources of "frame-overlap" neutrons, which are those arriving at a given time but originating from a different pulse and having a different wavelength than intended. For clarity the figures show these

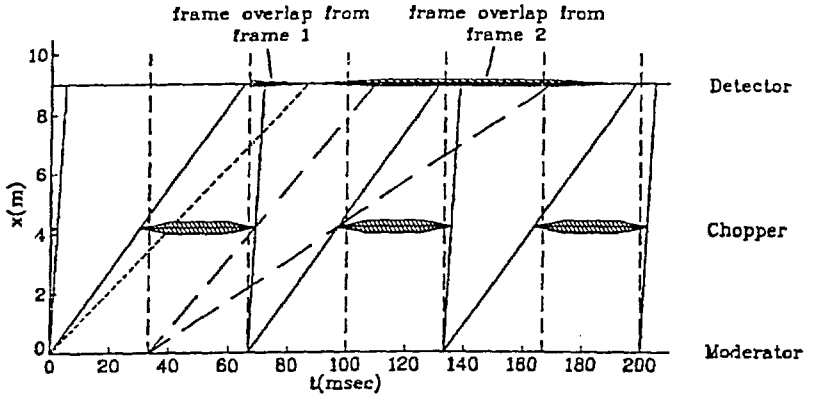

Figure 2. Time-distance diagram for a 20 cm dia drum chopper at 4.2 m from the source when the chopper is operating at 7.5 Hz and the source at 30 Hz. The broad hatched band at x=4.2 m indicates times when the chopper is fully-closed, and the regions where this band tapers to a point indicate times when the chopper is opening or closing, with the width of the band indicating the fraction of the beam blocked by the chopper. The chopper phasing and open-angle have been chosen to provide no interference for prompt frame-1 neutrons arriving at the detector between 5000 and 65000 μs when the chopper is operated at this frequency.

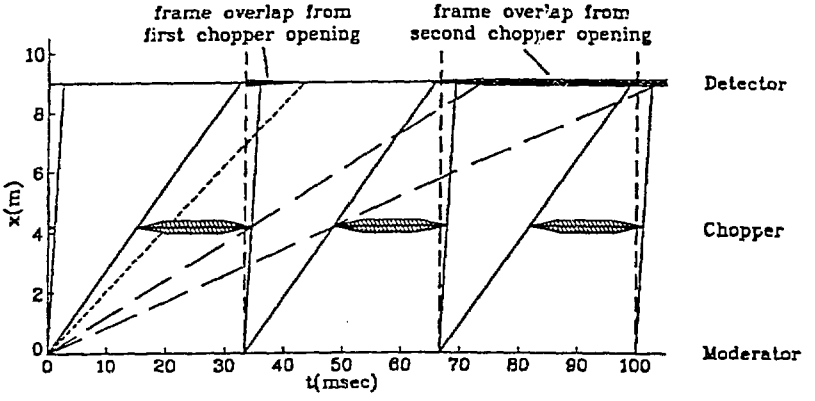

Figure 3. Time-distance diagram for the chopper of Fig. 2 operating at 15 Hz when the source operates at 30 Hz. Chopper open-angle is the same as for Fig. 3, but the chopper phasing has been changed to provide no interference for prompt neutrons arriving at the detector between 2500 and 32500 μs when the chopper is operated at this frequency.

frame-overlap neutrons as originating from only one or two of the prompt pulses, and arriving at the detector at times greater than 66667 μs or 33333 μs for Figs. 2 and 3 respectively. However, it should be remembered that the actual patterns repeat with periods of 66667 μs or 33333 μs (Figs. 2 or 3 respectively) so these "frame-overlap" regions can all be considered to collapse back onto the first 66667 μs for Fig. 2 or the first 33333 μs for Fig. 3.

Neutron trajectories could be selected from an energy distribution in one of two different modes. In the first mode, each neutron was given a random energy E according to the probability distribution

$$I(E) = AEe^{-E/E_0} + B/E[1 + (E/5E_0)^7] \qquad E < E_{max}$$
$$I(E) = 0 \qquad E > E_{max} \tag{2}$$

which is a Maxwellian joined to a 1/E epithermal spectrum with a Westcott joining function, and terminated at some maximum energy E_{max}. Each neutron was then randomly assigned to be "delayed" or "prompt" with relative probability given by the delayed-neutron fraction selected for that particular simulation. Prompt neutrons were randomly chosen to originate in frame-1 or frame-2 (with equal probabilities for 30 Hz source operation, or probability of 1 for frame-1 and 0 for frame-2 for 15 Hz source operation), and left the moderator at t=0 for frame-1 or at t=33333 μs for frame-2. Delayed neutrons left the moderator at a random time between t=0 and t=66667 μs. Each trajectory was inspected to see whether or not it was intercepted by the chopper. If intercepted, the neutrons were randomly "absorbed" or "transmitted" according to the absorption probability for the specified thickness of the absorbing material based on its linear absorption for neutrons of this energy. Each trajectory was also randomly detected or not detected by the detector, according to the assumed detector efficiency at this energy. Because of the form of the spectrum of Eq. (2), this mode resulted in the generation of a large number of trajectories for neutrons of high energies, but very few trajectories in the low-energy tail of the Maxwellian.

In the second mode, the neutron trajectories were chosen randomly from a uniform distribution of wavelengths extending over the range of 0-84 Å, which is three times the nominal range of the instrument. This wide range was chosen to reflect accurately the effects of frame-overlap neutrons on the simulated scattering spectra. Each trajectory was then weighted according to the probability of the occurrence of this wavelength in the original spectrum (Eq. 2) and assigned as above to frame-1, frame-2, or delayed. In this mode also, each trajectory was inspected to see whether or not it was intercepted by the chopper. If intercepted, the trajectory was weighted by the transmission probability for the specified thickness of the absorbing material based on its linear absorption for neutrons of this energy. Each trajectory was also weighted according to the detection probability for neutrons of this energy. This mode of trajectory generation, although requiring more computation time per trajectory than did the first mode, was much more efficient in sampling the long-wavelength behavior of the system. Thus this mode was used almost exclusively for the study reported here.

In either mode, each trajectory was binned according to the arrival time of the neutron at the detector. Arrival times greater than t=66667 μs were "wrapped-around" (had a multiple of 66667 μs subtracted from them to leave an arrival time between 0 and 66667) to provide a realistic treatment of frame-overlap. Each trajectory was actually accumulated into several different histograms, representing various combinations of the probabilities of transmission through the chopper and of detection.

Scattering by the Sample

The various spectra generated from the neutron trajectories as discussed above correspond to what would be called the incident beam "spectrum" in a small-angle diffraction measurement under the corresponding types of measurement conditions. In addition to these, a second set of spectra were accumulated in which the trajectories were weighted according to the probability of scattering from a sample and were binned according to arrival time (as above) and scattering angle. Scattering was assumed to be isotropic, and equal-width angular bins were chosen ranging between a specified minimum and maximum scattering angle. For each trajectory, the Q for scattering to the center of each angular bin was calculated, and the weight assigned to this bin was the scattering probability for each such Q multiplied by the solid angle of this bin ($2\pi\phi\Delta\phi$). Thus each trajectory contributed to scattering at every angle, but with a different probability for each angle. Use of such a fixed set of scattering angles rather than randomly selected scattering angles was dictated by the desire to generate a good statistical sampling of angles in a reasonable amount of computing time. This may have introduced some distortion into the data, but the results shown below indicate that any such distortion is small. The scattering probability assumed for all calculations reported here was that appropriate to the "Bates poly" sample used as a standard on SAD, namely

$$I(Q) = 0.0247\, Q^{-2}. \qquad (3)$$

Sample transmission was assumed equal to unity in generating these scattering spectra. All such scattering spectra were also weighted according to the probability of detection of each neutron, and two separate spectra were collected, one weighted according to the probability of transmission through the chopper and one corresponding to the no-chopper case.

The program REDUCE used for reduction of data from the SAD instrument was modified to give the program FEREDUCE to provide similar reduction of the scattering and spectral data output by FECHOPS. This program allowed a choice of which time-slices and angular bins were to be included in the data reduction, and then produced a "measured" I(Q) vs Q output file resulting from only this subset of the "raw" scattering data generated by FECHOPS.

III. SIMULATION RESULTS

The simulation program was run with a variety of parameters to investigate how such choppers might perform on the IPNS small-angle diffractometers. Parameters chosen were roughly those which would be appropriate to SAD or to the new small-angle diffractometer, and are summarized in Table I. For all calculations described here, the chopper was located in the beam gate cavity at 4.2 m from the moderator, and the detector was assumed to be 9.0 m from the moderator.

TABLE I - Parameters for the Simulations in Figures 4-9

Parameters varied	Figs. 4-5	Figs. 6-7	Figs. 8-9
Source frequency (Hz)	30	30	30
Chopper rotation freq (Hz)	7.5	7.5	15
Fully-open times at det (μs)			
t_{min}	5000	5000	2500
t_{max}	65000	65000	32500
Open-angle $2\delta\psi$ (rad)	1.7754	1.7754	1.7754
Delayed-neutron fraction	0.0	0.028	0.028

Parameters held fixed in all simulations

Moderator-chopper dist L_c (m)	4.2	Sample width (cm)	1.0
Moderator-sample dist L_s (m)	7.5	Minimum scattering angle (rad)	0.0
Moderator-detector dist L_d (m)	9.0	Maximum scattering angle (rad)	0.1
Moderator width (cm)	9.0	Number of scattering angle bins	50
Chopper radius R (cm)	10.0	Moderator spectral energy E_0 (meV)	3.0
Absorber material	B_4C	Thermal/epithermal ratio for moderator	3.0
Absorber thickness d (cm)	1.0	Maximum neutron energy (meV)	10^9
Detector thickness (cm)	2.5	Number of arrival time bins	200
^{3}He fill pressure (atm)	1.5	Number of trajectories	$3x10^6$

Frame-Elimination - Chopper at 7.5 Hz

Figure 4 shows the scattering detected from "Bates poly", calculated with the source running at 30 Hz and with no delayed neutrons, and Fig. 5 shows the "measured" incident beam spectrum (transmitted by chopper and detected) calculated under these conditions. The chopper was run at 7.5 Hz (15 Hz opening frequency) for these calculations. The chopper opening and phasing were chosen as in Fig. 2, so that frame-1 neutrons arriving at the detector between 5000 and 65000 μs had no chopper interference (the chopper was fully open, meaning that no portion of the chopper absorbing material was in the beam, when these neutrons passed the chopper position). Also shown for comparison in Fig. 4 is the "Bates poly" scattering function which was assumed in generating the simulated scattering data. In order to show more clearly the "instrumentally" introduced errors in the simulated scattering data, a plot of relative differences between the simulated results and the original "Bates poly" data is also included.

The most obvious deviation in Fig. 4 between the "measured" scattering function resulting from reducing the simulated scattering data and the original assumed scattering function ("Bates poly") is the "dip" in I(Q) between Q ~ 0.025 $Å^{-1}$ and Q ~ 0.04 $Å^{-1}$, which results from the relatively high-energy frame-2 prompt neutrons which were not rejected by the chopper. Figure 5 and the data printout from the simulation show clearly that only time-slices 101-112 (33331-37331 μs) were affected by such neutrons, and when these time-slices were eliminated from the analysis

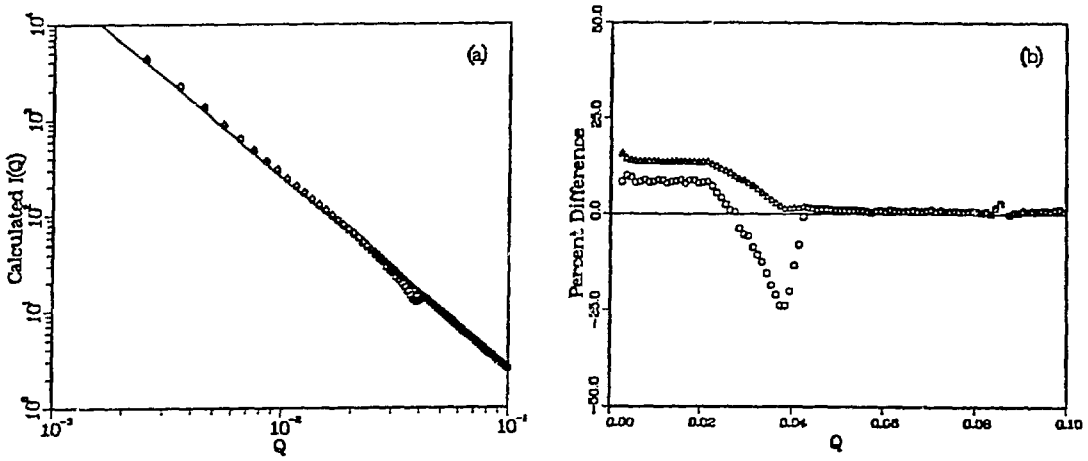

Figure 4. Reduction of simulated scattering data for Bates poly for 7.5 Hz chopper and 30 Hz source with no delayed neutrons. Chopper phasing and open-angle are as in Fig. 2. Other parameters of the simulation are given in Table I. (a) Full I(Q) calculated from the simulated data; (b) percent difference of the simulated I(Q) from the original scattering function. Angular bins between 0.004 and 0.1 rad and all time channels between 0 and 66667 μs were included in the analysis producing the circles, while time-channels between 33331 and 37331 μs were excluded from the analysis producing the triangles.

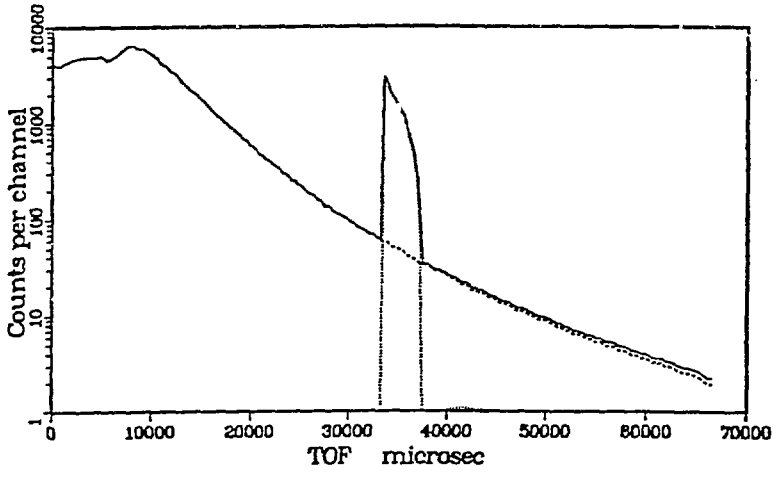

Figure 5. "Measured" spectra transmitted by the chopper and detected for the simulation of Fig. 4. The solid curve is the total spectrum, the dashed curve is the contribution from frame-1, and the dotted curve is the contribution from frame-2.

this deviation was gone from the resulting I(Q) vs Q curves (triangles in Fig. 4). However a more subtle deviation of the "measured" I(Q) from the assumed function still persisted over most of the small-Q portion of the data. This deviation was due to frame-overlap effects from frame-2 long-wavelength neutrons being transmitted through the chopper opening, as can be seen clearly in Fig. 2. Inspection of Fig. 2 suggested that this effect could be mostly eliminated if the chopper opening were designed to pass only the long-wavelength neutrons from frame-1 (say those arriving at the detector between 35000 and 65000 μs), and simulations under these conditions showed that this

was indeed the case, with quite good agreement between the resulting reduced data and the assumed scattering function. However, such a choice for chopper parameters means that several different chopper phasings would be required to cover the entire Q range, thus considerably reducing the effective data rate of the instrument. Alternatively, a suitable set of mirrors in the incident beam might be used to reflect out all wavelengths longer than ~28 Å and hence also eliminate such frame-overlap effects. Since such mirrors should provide only a small perturbation for wavelengths below 28 Å and would permit the full 28 Å range to be sampled with a single chopper setting, this would be the preferable alternative.

Figures 6-7 show data equivalent to that of Figs. 4-5, but this time with delayed neutrons included in the simulation. A delayed-neutron fraction of 0.028, appropriate to present IPNS operation as measured recently on SAD,[5] was assumed. Inspection of Fig. 7 shows that the chopper effectively eliminated those delayed neutrons which would have arrived at the longer times (above ~50000 μs) but did little to those which arrived at shorter times. This is evident in Fig. 6, where even after exclusion of the time-slices containing frame-2 prompt neutrons there is a large discrepancy between the measured and assumed scattering functions at intermediate Q values, while this discrepancy mostly disappears at low Q values. As shown in Fig. 6, these delayed-neutron effects can be largely eliminated by excluding time-slices 71-150 (roughly those where the delayed-neutrons contributed more than 10% of the incident spectrum) from the data reduction. Even with this large range of wavelengths (~10-21 Å) excluded, there is still sufficient redundancy in the data set to provide reduced data which completely cover the entire Q-range, although with somewhat poorer statistics. The resulting low-Q data are then in reasonable agreement with those of Fig. 4, indicating that most of the remaining low-Q discrepancies are due to frame-overlap effects. There are still some remaining delayed-neutron effects at intermediate Q values in the

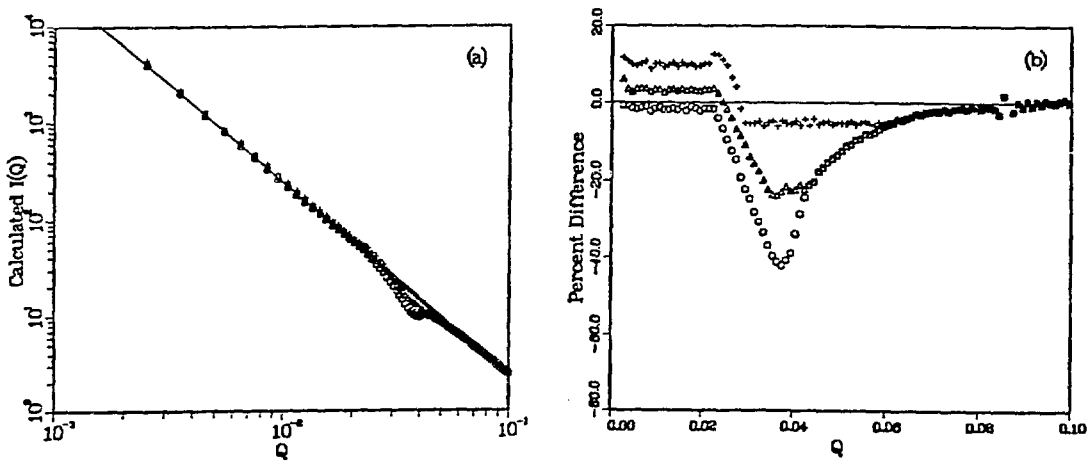

Figure 6. Reduction of simulated scattering data for Bates poly for 7.5 Hz chopper and 30 Hz source with a delayed-neutron fraction of 0.028. Chopper phasing and open-angle are as in Fig. 2. Other parameters of the simulation are given in Table I. (a) Full I(Q) calculated from the simulated data; (b) percent difference of the simulated I(Q) from the original scattering function. Angular bins between 0.004 and 0.1 rad and all time-channels between 0 and 66667 μs were included in the analysis producing the circles, while time-channels between 33331 and 37331 μs were excluded from the analysis producing the triangles and time-channels between 23331 and 50000 μs were excluded from the analysis producing the pluses.

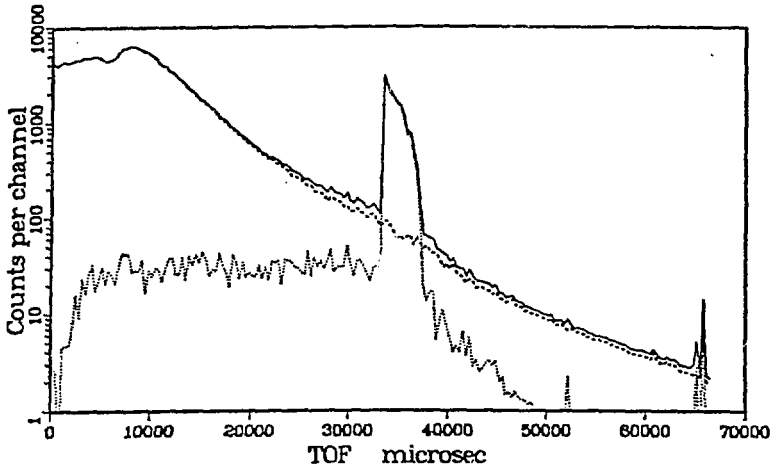

Figure 7. "Measured" spectra transmitted by the chopper and detected for the simulation of Fig. 6. The solid curve is the total spectrum, the dashed curve is the contribution from frame-1, and the dotted curve is the contribution from frame-2.

reduced data, but these result in less than 10% errors (consistent with the choice of time-slices for exclusion) which can be readily handled with analytical correction techniques.[5,6]

Delayed-Neutron-Elimination - Chopper at 15 Hz

Instead of operating the chopper at 7.5 Hz to eliminate alternate prompt pulses, the same chopper can be operated at 15 Hz while utilizing every pulse of the 30 Hz source. In this case the maximum wavelength is restricted to ~14 Å. Figure 3 shows the distance-time diagram which results when the chopper of Fig. 2 is operated at 15 Hz (thus opening and closing at 30 Hz) and phased to provide clear transmission for neutrons arriving at the detector between 2500 and 32500 μs. Figures 8-9 show simulated results with this chopper system when the delayed-neutron fraction was set to 0.028. In Fig. 8, the data are in good agreement with the assumed function except at the lowest Q values where the data lie somewhat above the assumed function. Inspection of Fig. 3 indicates that this is most likely due to frame-overlap. Additional simulations with no delayed neutrons showed data essentially identical to those of Fig. 8, confirming that the chopper had eliminated all significant delayed-neutron effects from the reduced data. This is supported by Fig. 9, which shows that the chopper had indeed eliminated essentially all the delayed neutrons in the incident spectrum which would have arrived at the longer times where the scattering signal and the prompt incident spectrum were small. The chopper passed the delayed neutrons at shorter times, but there the scattering signal and the spectrum were sufficiently large that the delayed neutrons had relatively little effect on the resulting reduced scattering data.

By changing the phase of this same chopper while still operating at 15 Hz, it can be used in a "band-selecting" mode where it is set to pass neutrons arriving at the detector between 35000 and 65000 μs after each pulse, thus covering the long-wavelength part of the range considered in Figs.

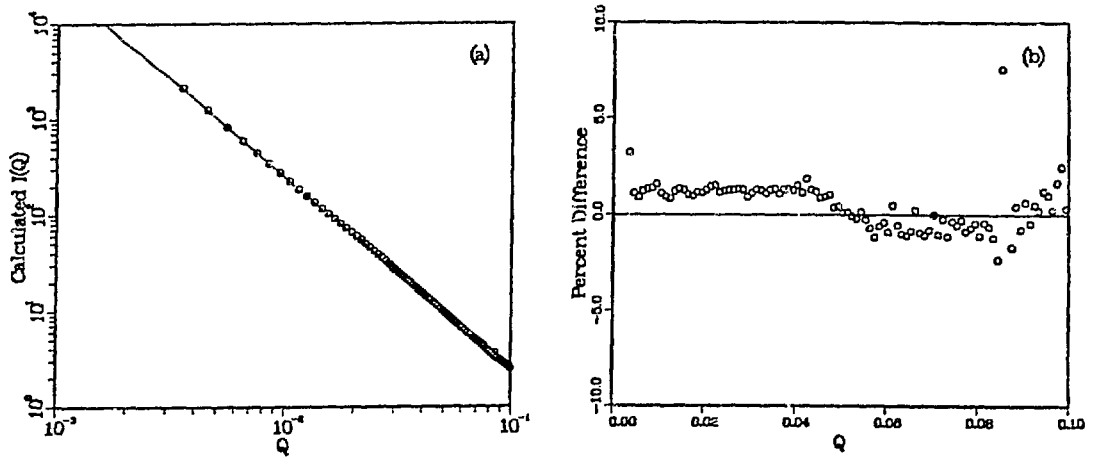

Figure 8. Reduction of simulated scattering data for Bates poly for 15 Hz chopper and 30 Hz source with a delayed-neutron fraction of 0.028. Chopper phasing and open-angle are as in Fig. 3. Other parameters of the simulation are given in Table I. (a) Full I(Q) calculated from the simulated data; (b) percent difference of the simulated I(Q) from the original scattering function. Angular bins between 0.004 and 0.1 rad and all time-channels between 0 and 33331 μs were included in the analysis.

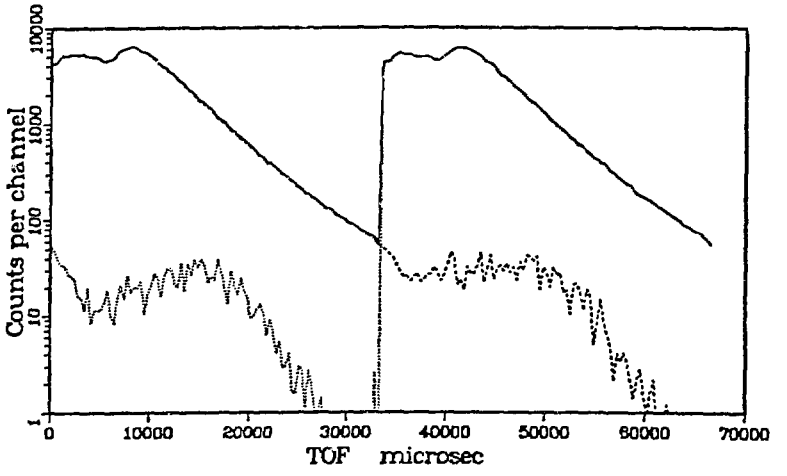

Figure 9. "Measured" spectra transmitted by the chopper and detected for the simulation of Fig. 8. The solid curve is the total spectrum, the dashed curve is the contribution from frame-1, and the dotted curve is the contribution from frame-2.

4-7 but using every pulse. However, inspection of Fig. 3 shows that this is likely to lead to problems. Any choice of chopper phasing other than that shown in Fig. 3 leaves the chopper open at the times these long-wavelength neutrons reach the detector, and thus allows faster delayed neutrons to reach the detector at these same times. Further simulations with such chopper phasing showed that, as expected, virtually all the long-wavelength portion of this spectrum was overwhelmed either by frame-2 prompt neutrons (shorter-wavelength portion of this band) or by delayed neutrons (longer-wavelength portion of the band). Thus it does not appear likely that

different choices of chopper phase (other than those near that shown in Fig. 3) will yield significant amounts of useful long-wavelength data.

Operation at Short Wavelengths - Chopper at 60 Hz

The time required for the chopper to go from fully open to fully closed is the time required for one edge of the chopper opening to sweep through half the beam width, since the exit side of the chopper will be sweeping through the other half of the beam at the same time. For a 20 cm diameter chopper operating at 15 Hz and chopping a 4.52 cm wide beam (this is the beam width at the 4.2 m chopper location in these simulations), this time required to go from fully open to fully closed or *vice versa* is 2419 μs. This translates to a 5183 μs range of times at the detector associated with neutrons which have passed through the partially open chopper (tapered portion of the shaded chopper band in Fig. 3). If this chopper is phased to begin opening at time t=0, then the first neutrons for which it is fully open are those arriving at the detector at t=5183 μs, which have λ=2.28 Å. In order to have the chopper be fully closed at t=0 and fully open for shorter-wavelength neutrons, it must be operated at a higher speed. This in turn will reduce the maximum wavelength which it will transmit.

Simulations were carried out for the case when the chopper was operating at 60 Hz (opening and closing at 120 Hz) and was phased to be fully open for neutrons detected at 1200 μs (starting to open at -96 μs). With this phasing the chopper was fully open for neutrons detected between 1200 and 8700 μs (0.53-3.82 Å) and after one-half revolution was again fully open for neutrons detected between 19057 and 26557 μs (8.38-11.67 Å). Analyzing only the data from time-frames corresponding to these two full-transmission regions lead to excellent agreement with the original scattering law, so it may be useful sometimes to operate the chopper at these higher frequencies when short-wavelength neutrons are desired. However, even with 60 Hz operation it does not appear feasible to utilize neutrons much below 0.5 Å without rephasing to let some of the initial fast burst through the chopper, and this may lead to background and detector-recovery problems. Also, with 60 Hz operation, roughly half of the potentially useful wavelengths are discarded by the chopper, so this mode is not very efficient.

IV. SEMI-QUANTITATIVE COMPARISON OF INTENSITIES

The intensity I measured in a solid angle $d\Omega$ and wavelength interval $d\lambda$ from a sample with cross-section $d\Sigma/d\Omega$ is

$$I = I_0 A_s t_s T_s \epsilon (d\Sigma/d\Omega)\, d\Omega d\lambda \qquad (4)$$

where I_0 is the total intensity per unit wavelength on the sample of area A_s and thickness t_s, T_s is the sample transmission, and ϵ is the detection efficiency. If converging multiple-aperture collimators are used and the distances from source-to-sample and sample-to-detector are kept fixed, then the intensity on the sample will vary at least as fast as $\Delta\alpha^2$, where $\Delta\alpha$ is the incident beam divergence permitted by a single channel of the collimators, assuming the collimators are ideal

(zero blade thickness).[7] If a chopper is used to remove n-1 pulses out of every n pulses, then the incident beam intensity at a given wavelength will be proportional to 1/n. With these assumptions, and considering only the long-wavelength λ^{-5} portion of the incident beam spectrum

$$I_o \propto n^{-1} \lambda^{-5} \Delta\alpha^2 . \tag{5}$$

The size of the penumbra of the direct beam at the detector determines the minimum useful scattering angle $2\theta_{min}$, and this penumbra size is nearly linearly related to $\Delta\alpha$, so to a reasonable approximation

$$\Delta\alpha \propto \theta_{min} . \tag{6}$$

When the instrument is configured for a specific Q_{min}, and Q is measured for a specific combination of θ, λ, $\Delta\theta$ and $\Delta\lambda$, the measured intensity is thus

$$I(Q \geq Q_{min}) \propto (d\Sigma/d\Omega)\, n^{-1} \lambda^{-5} \theta_{min}^2 \, d\Omega d\lambda . \tag{7}$$

At some small $Q = Q_{min}$ we must have $\theta = \theta_{min}$ and $\lambda = \lambda_{max}$, since

$$Q_{min} \propto \theta_{min}/\lambda_{max} , \tag{8}$$

and to provide appropriate resolution

$$\Delta\theta \propto \theta_{min} \tag{9}$$

$$\Delta\lambda \propto \lambda_{max} . \tag{10}$$

Furthermore, for isotropic scattering

$$d\Omega \propto \theta \, \Delta\theta \propto \theta_{min}^2 . \tag{11}$$

Combining these results in the relationship

$$I(Q=Q_{min}) \propto (d\Sigma/d\Omega)\, n^{-1} Q_{min}^4 . \tag{12}$$

Thus with the approximations made here, the measured intensity at Q_{min} for a given Q_{min} depends only on n, and is highest (n=1) when Q_{min} is achieved by tightening the collimation rather than by eliminating pulses. However this dependence is only first order, and when the realities of practical converging multiple-aperture collimator construction (such as blade thicknesses on soller collimators) are taken into account it is likely that the two approaches would yield intensities of comparable magnitude at a Q_{min} of ~0.002 $Å^{-1}$, which is the goal for the new IPNS small-angle diffractometer.

V. DISCUSSION

These simulation results showed that a drum chopper of the type described in Fig. 1 and Table I operating at 7.5 Hz could be effective in the elimination of most of the prompt neutrons from the second frame, permitting collection of data with neutrons out to ~28 Å on the IPNS small-angle diffractometers. The same chopper operating at 15 Hz could eliminate most delayed-neutron effects from the data obtained with normal 30 Hz source operation which utilizes neutrons out to ~14 Å, thus resulting in much better signal-to-noise than is currently available on SAD for the long-wavelength data. However, when the chopper was operated at 7.5 Hz in the simulation both delayed-neutron and frame-overlap problems were evident in the data. The delayed neutron effects were mostly eliminated in this case by rejection of time-slices arriving at times between ~24000 and ~50000 μs. The frame-overlap effects could be mostly eliminated by use of a chopper with a narrower opening (which would then restrict the Q-range which could be covered with one setting), or possibly by other means such as critical reflection from suitably-arranged mirrors.

The geometries of SAD and and the new IPNS small-angle diffractometer are somewhat restrictive with regard to use of such a chopper. All the simulations reported here have been for a chopper at 4.2 m from the source, which corresponds to the gate cavity location for these instruments. The chopper diameter was therefore set at 20 cm, which is roughly what would fit in this cavity. Some simulations were also carried out with the chopper located just outside the biological shield (5.65 m from the source). As would be expected from Fig. 2, this mode of operation was much less satisfactory, with much more of the frame-2 prompt pulse being transmitted, and agreement between reduced data and the assumed scattering function was not achieved for the limited number of situations simulated with this chopper distance. (Agreement could probably be achieved if the chopper opening were made sufficiently narrow, but this would lead to other operational problems.)

Semi-quantitative arguments comparing the options of tightening collimation or using longer wavelengths to reach smaller Q values, indicate that tightening collimation appears to give a higher intensity near Q_{min}. Many details such as the minimum resolution achievable on the detector, the non-zero thickness of the collimator blades, *etc.*, have been ignored in obtaining this rough estimate. As the collimation is pushed to smaller values of $\Delta\alpha$, collimator blade thickness will start to become important, and detector resolution will become important when θ_{min} or the $\Delta\theta$ necessary at θ_{min} are reduced to values comparable to the detector resolution divided by the sample-detector distance. For the small-angle diffractometers at the 30 Hz IPNS source, both of these effects become important below Q_{min} ~0.003 $Å^{-1}$. Thus the approximate intensity relationship derived above should be considered to be merely a rough guide, but the conclusions should still be valid; namely that the use of a frame-eliminating chopper of the type considered appears to be feasible, at least in terms of intensities, and that the use of such a chopper probably would result in data rates comparable to those which would be obtained if tighter collimation alone were used to achieve the same small values of Q_{min}.

If a frame-elimination chopper were used, it would be relatively simple to stop it in the open position or to have it open at the 30 Hz rate (rotation at 15 Hz), thus setting n=1 and giving one particular value of Q_{min}. It would then be quite easy to change the chopper opening rate to 15 Hz

(rotation at 7.5 Hz) to give n=2 and a factor of 2 reduction in Q_{min} with the same collimators. Changing between Q_{min} values in this fashion should be much simpler than the elaborate automated collimator and beamstop insertion mechanisms which would be required to vary $\Delta\alpha$ to change Q_{min}.

In conclusion, the simulations have shown that a chopper of the type considered would make a significant improvement in the signal/background at the IPNS small-angle scattering instruments. It would also provide much greater flexibility and the option of using, when the need arises, longer-wavelength neutrons than would otherwise be possible. Thus the IPNS small-angle-scattering instruments will be equipped with such choppers as soon as is practical. Similar choppers would likely be beneficial on other pulsed-source small-angle-scatering instruments as well.

APPENDIX 1 - Drum Chopper Description

Chopper Phase and Opening Angle

The chopper is designed to be completely open for prompt neutrons arriving at the detector at times between t_{min} and t_{max}. If the total flight path to the detector is L_d, then the chopper must be completely open between t_{cmin} and t_{cmax} given by

$$t_{cmin} = (L_c/L_d)t_{min} \tag{A1}$$

$$t_{cmax} = (L_c/L_d)t_{max}\,. \tag{A2}$$

If the beam is designed to have a width W_m at the moderator and W_s at the sample, then its width W_c at the chopper is

$$W_c = [W_s L_c + W_m(L_s - L_c)]/L_s\,, \tag{A3}$$

where L_c and L_s are defined in Fig. 1. This width translates into an angular chopper opening of

$$\delta\psi_w = 2\sin^{-1}(W_c/2R) \tag{A4}$$

where R is the chopper radius (Fig. 1). Between the times t_{cmin} and t_{cmax} the chopper rotates through an angle

$$\delta\psi_r = \omega(t_{cmax} - t_{cmin}) \tag{A5}$$

where ω is the angular rotational frequency of the chopper. The total chopper opening angle (Fig. 1b) is then

$$2\delta\psi = \delta\psi_w + \delta\psi_r\,. \tag{A6}$$

The center of the chopper opening must be lined up with the beam axis at the time t_c given by

$$t_c = (t_{cmax} + t_{cmin})/2 . \quad (A7)$$

Interception of Neutrons

The neutron is emitted at time t_e from the position y_m on the moderator. It then travels with velocity v at an angle α to the beam centerline (Fig 1b). The chopper is a hollow cylindrical drum, which can be treated as a thin shell of radius R rotating with angular frequency ω if the thickness of the absorbing material is small compared to R. The chopper has openings on opposite sides, each of which subtends an angular range, at the chopper center, of $\pm\delta\psi$ about a line through the centers of these two openings. The chopper axis is located at $x=L_c$, $y=0$, and the chopper phase is such that the center of the chopper openings lines up with the beam centerline at time t_c.

The neutron trajectory makes two intersections with the chopper shell or its openings. These are at positions (x_1,y_1) and (x_2,y_2), shown in Fig. 1b. If α is assumed to be small, it can be shown that for i=1 or i=2

$$x_i = L_c - [B - (-1)^i D]/A \quad (A8)$$

$$y_i = y_m + \alpha x_i , \quad (A9)$$

where

$$A = 1 + \alpha^2 \quad (A10)$$

$$B = \alpha(y_m + \alpha L_c) \quad (A11)$$

$$D = \{\alpha^2(y_m + \alpha L_c)^2 - (1 + \alpha^2)[(y_m + \alpha L_c)^2 - R^2]\}^{1/2} . \quad (A12)$$

These two intersections occur at the times t_1 and t_2 given by

$$t_i = t_e + [x_i^2 + (y_i - y_m)^2]^{1/2}/v . \quad (A13)$$

The points (x_1,y_1) and (x_2,y_2) can be represented as the points (R,ψ_1) and (R,ψ_2) in a polar coordinate system centered on the chopper axis.

$$\psi_i = \tan^{-1}[y_i/(x_i - L_c)] + (i-2)\pi . \quad (A14)$$

In this same coordinate system at time t_i the two chopper openings are centered at (see Fig. 1b)

$$\psi_{cai} = \omega(t_i - t_c) - \pi \quad (A15)$$

$$\psi_{cbi} = \omega(t_i - t_c) . \quad (A16)$$

For a "black" chopper, the neutron will be transmitted at its i^{th} intersection with the chopper periphery if it lines up with either opening, or hence if for some integer n

$$\psi_{cai} - \delta\psi \pm 2n\pi < \psi_i < \psi_{cai} + \delta\psi \pm 2n\pi \qquad \text{(A17)}$$

or if

$$\psi_{cbi} - \delta\psi \pm 2n\pi < \psi_i < \psi_{cbi} + \delta\psi \pm 2n\pi \,. \qquad \text{(A18)}$$

In order for the neutron to reach the sample, it must be transmitted for both i=1 and i=2.

If the chopper is not "black", there is some probability of transmission even if the neutron is intercepted by the chopper. This can be easily computed from the linear absorption coefficient of the absorbing material and its thickness, and on whether the trajectory of the neutron traverses this thickness once or twice.

References

1. J. M. Carpenter. Nucl. Instr. and Meth. 145, 91-113 (1977).
2. J. M. Carpenter. Nucl. Instr. and Meth. 175, 287-292 (1980).
3. B. S. Brown, J. M. Carpenter, R. K. Crawford, A. V. Rauchas, A. W. Schulke, and T. G. Worlton. Advanced Neutron Sources 1988, Proceedings of the 10th Meeting of the International Collaboration on Advanced Neutron Sources (ICANS X), held at the Los Alamos National Laboratory, Oct. 3-7, 1988. Institute of Physics Conference Series Number 97, IOP Publishing Ltd, New York. pp 27-45 (1989).
4. R. K. Crawford. Unpublished notes (1986).
5. J. E. Epperson, J. M. Carpenter, P. Thiyagarajan, and B. Heuser. Nucl. Instr. and Meth. A289, 30-34 (1990).
6. J. M. Carpenter, D. F. R. Mildner, J. W. Richardson, Jr., and W. Dimm. "Correcting Beam Monitor and Diffraction Data for Chopped Delayed Neutron Backgrounds", these proceedings.
7. R. K. Crawford and J. M. Carpenter. J. Appl. Cryst. 21, 589-601 (1988).